Available online at www.sciencedirect.com
ScienceDirect
Trans. Nonferrous Met. Soc. China 31(2021) 1249−1261
Transactions of Nonferrous Metals Society of China
www.tnmsc.cn

Influence of TiB_2 addition on friction and wear behaviour of Al2024−TiB_2 ex-situ composites

Dipankar DEY, Abhijit BHOWMIK, Ajay BISWAS

Mechanical Engineering Department, NIT Agartala, Tripura-799046, India

Received 18 May 2020; accepted 20 October 2020

Abstract: Present work encapsulated the friction and wear behaviour of aluminium matrix composites reinforced with different mass fractions of titanium diboride (TiB_2) particles, synthesized by stir casting. A pin on disc tribotester was employed for conducting the dry sliding wear tests of Al2024−TiB_2 composites. The tests were performed adopting various parameters like load, sliding distance and sliding velocity for investigating the effect of tribological parameters on the prepared composites. Microstructural characterization confirmed uniform dispersion of TiB_2 particles and good matrix−reinforcement bonding. Results of the experiments revealed that, low friction and wear rates were observed in the developed composites compared to Al2024 alloy, whereas wear rates of both Al2024 alloy and fabricated composites increased with the increase in load, sliding velocity and sliding distance. However, friction coefficient of both Al2024 alloy and fabricated composites reduced with the increase in applied load but rose with the increase in sliding velocity and sliding distance. SEM studies of the worn surfaces and debris depicted that enhancement in wear resistance can be ascribed to finer debris formation.

Key words: Al2024 alloy; TiB_2; stir casting; friction; wear

1 Introduction

Aluminium matrix composites (AMCs) are one of the most promising materials nowadays possessing remarkable properties such as good thermal conductivity, high strength, wear resistance, corrosion resistance and these properties make AMCs an appealing material for various automotive and aerospace applications [1−4]. Properties of particulate reinforced AMCs are mainly influenced by type, size and quantity of reinforcements; and uniform dispersion of reinforcement results in enhancement of mechanical and tribological properties [5]. Hard ceramic particles like Al_2O_3 [6], TiC [7], SiC [8], TiB_2 [9] and B_4C [10] are commonly employed as reinforcements for enhancing the mechanical and tribological properties of AMCs. Among these, TiB_2 emerged to be the most promising reinforcement as it possesses high hardness, high stiffness and most importantly, it does not react with molten aluminium alloy to generate any detrimental by-product at the matrix−reinforcement interfaces [11]. Further, TiB_2 also contributes to the wear resistance of AMCs. Sound interfacial bonding between TiB_2 and Al enhances the hardness, which augments the wear resistance of Al−TiB_2 composites [12]. Al2024 alloy is basically a wrought alloy consisting of copper as the primary alloying element, possessing excellent fatigue resistance, high strength, good machining properties and extensively used in screw machine products, aircraft structures, automobile engines, orthopaedic equipment and rivets. However, Al2024 has some limitations in terms of tribological properties. Therefore, it is necessary to develop a composite possessing enhanced wear resistance without negotiating its strength [13,14].

Corresponding author: Dipankar DEY, E-mail: deybulton@gmail.com
DOI: 10.1016/S1003-6326(21)65575-9

Adaptation of appropriate technique for AMC fabrication involves numerous challenges like matrix−reinforcement compatibility, uniformity in reinforcement distribution, grain refinement, clear interface and bonding characteristics [15]. AMCs can be synthesized by many techniques like powder metallurgy, stir casting, centrifugal casting, severe plastic deformation, diffusion bonding, and friction stir processing [16−18]. Among them, stir casting is an effective production technique as it provides a wide choice of materials and conditions for production and is comparatively cheap [19,20].

Fabrication and tribological performances of Al−TiB_2 composites were extensively reported in Refs. [19−29]. PORIA et al [19] investigated the hardness and wear behaviour of LM4−TiB_2 composites by adopting various loads and sliding speeds and stated that, inclusion of TiB_2 particles into aluminium alloy increases the hardness as well as wear resistance capacity of LM4−TiB_2 composites significantly. JOHNY JAMES et al [21] compared the mechanical and wear properties of aluminium matrix composites reinforced with SiC and TiB_2 particles and revealed that, TiB_2-reinforced composites exhibit higher strength and wear resistance than SiC-reinforced composite. TJONG and LAU [22] fabricated Al−TiB_2 composites by powder metallurgy and observed that by the inclusion of 20 vol.% titanium diboride particles into Al−4Cu alloy, dry sliding wear resistance is improved noticeably. RADHIKA and RAGHU [23] fabricated Al−TiB_2 composites by centrifugal casting using LM13 aluminium alloy as matrix and concluded that, applied load was the most important factor influencing wear behaviour. MAHAMANI et al [24] synthesized AA6061−TiB_2/ZrB_2 composites by flex-assisted synthesis process and observed enhancement in mechanical and tribological properties of the fabricated composites compared to matrix alloy. The analysis of SURESH and MOORTHI [25] revealed that, incorporation of TiB_2 into AA6061 alloy resulted in enhancement of mechanical and tribological properties. In another study by MANDAL et al [26], influence of TiB_2 addition on wear behaviour of Al−4Cu alloy was analyzed and they concluded that, an increase in TiB_2 content results in an increase in wear resistance. KUMAR et al [27] produced in situ Al−7Si/TiB_2 composites by K_2TiF_6−KBF_4 reaction at 800 ºC and reported that, uniform dispersion of TiB_2 particles and good matrix−reinforcement interfacial bonding were achieved. Experimental results further revealed that the incorporation of TiB_2 particles resulted in significant improvement of mechanical properties and wear resistance followed by reduction in friction coefficient compared to the matrix alloy. RAMESH and AHAMED [28] conducted friction and wear analysis of in situ AA6063−TiB_2 composites by varying the load, sliding velocity and sliding distance. Outcome of the experiments revealed that, low friction and wear rates were observed in the developed composites compared to unreinforced alloy, whereas wear resistance of both unreinforced alloy and composites reduced with the increase in applied load, sliding velocity as well as sliding distance. ZHAO et al [29] compared the wear resistance of TiB_{2P}/Al and SiC_P/Al composites synthesized by squeeze casting and stated that, TiB_{2P}/Al composite exhibited an increase in wear resistance followed by the reduction in friction coefficient as compared to SiC_P/Al composite. However, there are no literatures covering comprehensive studies of the impact of titanium diboride addition on friction and wear behaviour of Al2024 alloy composites fabricated by stir casting.

Al2024 alloy is one of the hardest aluminium alloy and TiB_2 also possesses high hardness. The main aim of this work was to use the combined effect of hardness of both Al2024 alloy and TiB_2 for improving the wear resistance capacity of Al2024 alloy for various tribological applications and to investigate the effect of various tribological parameters on dry sliding wear and friction behaviour of Al2024−TiB_2 composites.

2 Experimental

Chemical composition of base metal (Al2024 alloy) used in the present study is illustrated in Table 1. TiB_2 powder having a purity of greater than 99% and size of 13−14 μm was used as reinforcement. The AMCs were made using 0, 3, 6 and 9 wt.% of micro TiB_2 powders. Density of Al2024 alloy was 2.78 g/cm^3 and that of TiB_2 particles was 4.52 g/cm^3. Composites were fabricated using an induction furnace equipped with a mechanical stirrer by means of stir casting method. At first, small pieces of measured quantity of Al2024 alloy was heated to 650 °C in a graphite

crucible. TiB_2 powders were preheated at 450 °C for 30 min in a distinct muffle furnace to discard away the moisture and then added to the melt. 2% magnesium was also introduced into the melt to increase the wettability. The mixture was then stirred at 350 r/min for 10 min to ensure even distribution of TiB_2 particles. Subsequently, the mixture was poured into a preheated mould and allowed to cool at ambient temperature. Then, the solidified metal was separated from the mould and machined correctly for conducting wear and friction analysis.

Table 1 Chemical composition of Al2024 alloy (wt.%)

Fe	Si	Mg	Mn	Cu	Zn	Ti	Cr	Al
0.5	0.5	1.5	0.8	4.1	0.25	0.15	0.1	Bal.

The microstructural characterization of the prepared composites was accomplished using SEM with EDS. A pin on disc tribotester (Model: Ducom TR 20LE-M5) was employed for carrying out the wear tests of Al2024−TiB_2 composites, for analyzing the friction and wear behaviour. All the tests were performed at room temperature (20−25 °C). Cylindrical pins (from both matrix and fabricated composites) of 6 mm in diameter and 40 mm in length were used for conducting the tests. For attainment of uniformity in surface roughness of all the pins, sliding faces of the pins were polished with emery paper of 200, 400 and 600 grit, respectively. The pins were made to slide against a hardened steel disc (EN31 material) with hardness of 62 HRC. For all the tests, a track diameter of 8 cm was used. Before starting of every experiment, the counter disc and pin sliding faces were washed with acetone to eliminate the footprint of foreign materials. The tests were carried out in three sets, combining different loads (10, 20 and 30 N), sliding distances (900, 1800 and 2700 m) and sliding velocities (0.5, 1.0 and 1.5 m/s). After every test, the volume loss was determined using Eq. (1):

$$V=\pi r^2(l_i-l_f) \quad (1)$$

where V is the volume loss, r is the pin radius, l_i is the pin length before testing and l_f is the pin length after testing. In order to establish confidence in the experimental results, all the tests were repeated three times. During all the experiments, the frictional force was recorded by means of a data acquisition system attached to the tribotester for determining the friction coefficient. After the tests, wear tracks and debris were analyzed using SEM.

3 Results and discussion

3.1 Microstructure

Figure 1 represents the SEM images and EDS spectrum of the developed Al2024−TiB_2 composites. Figure 1(a) displays the SEM micrograph of unreinforced material (Al2024 alloy). Figures 1(b−d) show that the developed composites are compact and also confirm uniform dispersion of TiB_2 particles, thus establishing good matrix−reinforcement bonding. Figure 1(d) also depicts that the shape of TiB_2 particles is either hexagonal or spherical. All the SEM micrographs demonstrate unavailability of casting defects like micro cracks, porosity, slag inclusion and shrinkage, thus confirming the accomplishment of excellent quality of casting. All these properties together help to enhance the tribological behaviour of the prepared composites. The EDS spectrum of Al2024−9%TiB_2 composite is presented in Fig. 1(e). Peaks of B and Ti were spotted in the spectrum which endorses the existence of TiB_2 in Al2024−9%TiB_2 composite.

Figure 2 displays the EDS mapping of Al2024−6%TiB_2 composite. It clearly shows the existence of Ti and B in the fabricated composite, which are were uniformly distributed within the matrix.

3.2 Wear behavior

3.2.1 Impact of load

Wear tests were performed at three different loads (10, 20 and 30 N), keeping the sliding velocity and sliding distance constant at 1.5 m/s and 1800 m, respectively. Figure 3 shows the influence of load on volume loss of Al2024−TiB_2 composites. From Fig. 3, it can be observed that, with the increase in load, volume loss of Al2024−TiB_2 composites increases and the behaviour is approximately concave except for Al2024−6%TiB_2 composite. The increase in load leads to high contact pressure and generation of high frictional heat between the pin sliding face and disc, resulting in plastic deformation. A higher degree of plastic deformation may cause sub-surface cracking of pin, leading to higher material removal [5,24]. The rise in wear rate at higher loads can be attributed to

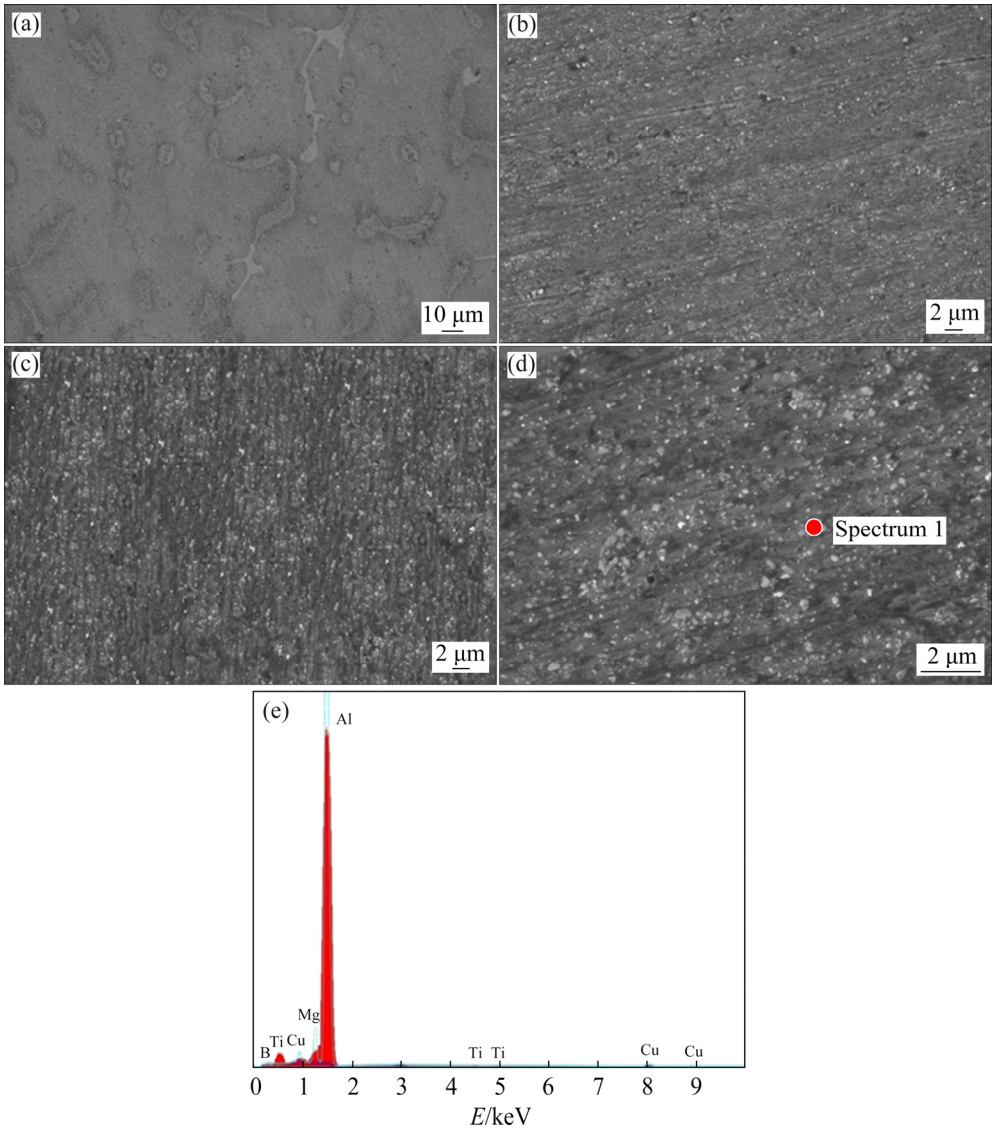

Fig. 1 SEM images of Al2024−0%TiB_2 (a), Al2024−3%TiB_2 (b), Al2024−6%TiB_2 (c), Al2024−9%TiB_2 (d) (at higher magnification) composites, and EDS spectrum of Al2024−9%TiB_2 composite (e)

delamination, abrasion and chipping out of TiB_2 particles from the matrix. At a higher load of 30 N, abrasion occurs in which hard asperities of reinforcement particles lying between the sliding faces, cut and plough the pin, resulting in higher wear rates. Delamination consists of propagation and nucleation of cracks, and the rise in load accelerates these phenomena and increases wear [30]. Figure 3 further depicts that volume loss of Al2024 alloy is more than that of the fabricated composites under all load conditions. The increase in TiB_2 mass fraction increases the hardness, which boosts up the load-bearing capacity, as this emergence of adhesive processes is delayed by increasing the mating metal hardness [28]. Uniform distribution of TiB_2 particles resists the plastic deformation of asperities. This results in oxide formation on newly exposed surface. Wear loss of matrix material is significantly quicker until the contact of oxide film comes into play. In the case of unreinforced material, the plastic deformation of asperities is very high so that the newly exposed surface does not have enough time for oxide film growth, resulting in the increase in wear rate of unreinforced material. Another important phenomenon for decreased wear resistance in the case of unreinforced materials is adhesion of debris to sliding surfaces of the steel disc and pin and with prolonged sliding action, and these small asperities take the shape of bigger asperities, penetrate the pin surfaces, resulting in greater wear. But for Al2024−TiB_2 composites, reinforcement particles resist the

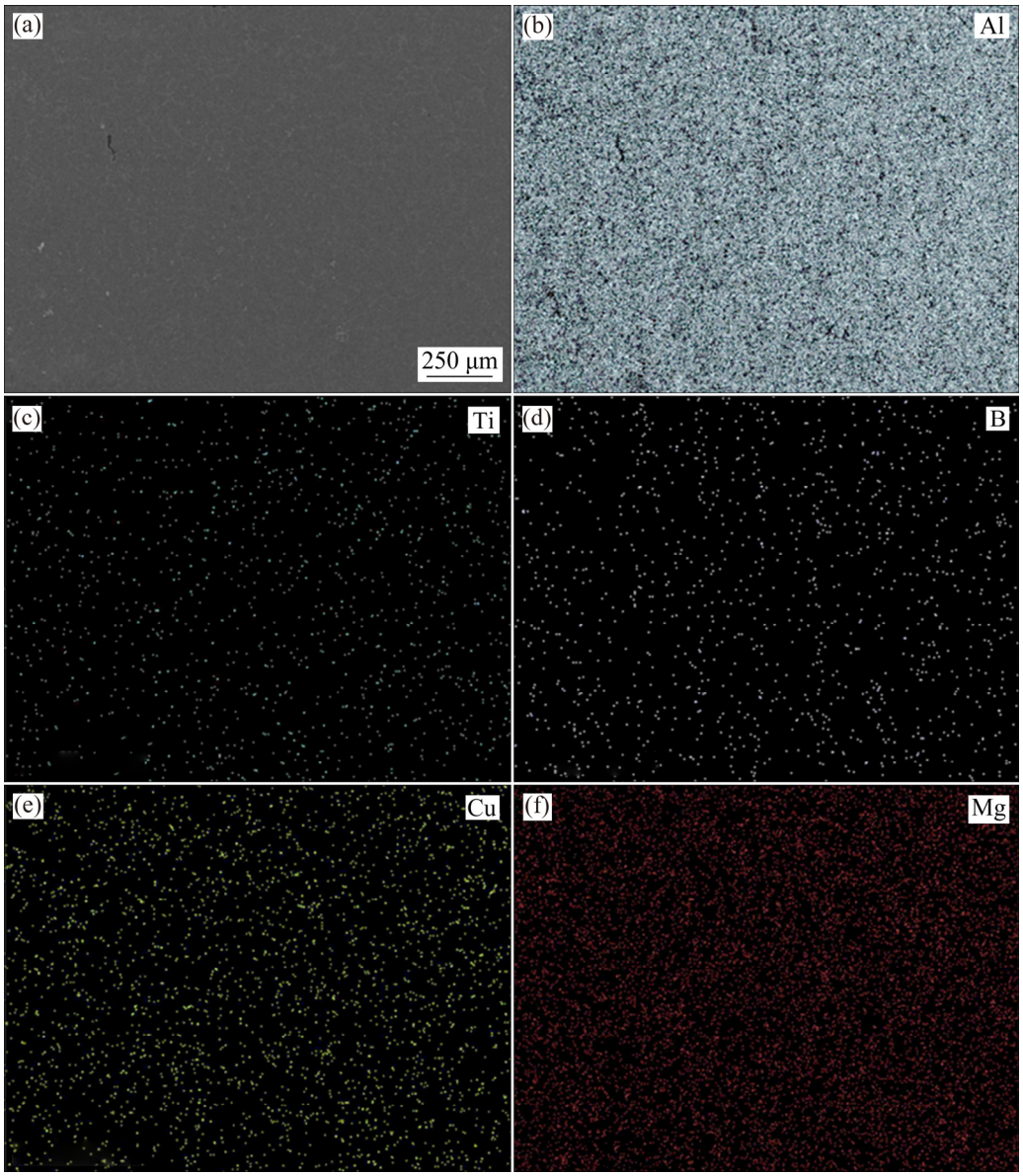

Fig. 2 EDS mapping results of Al2024−6%TiB_2 composite

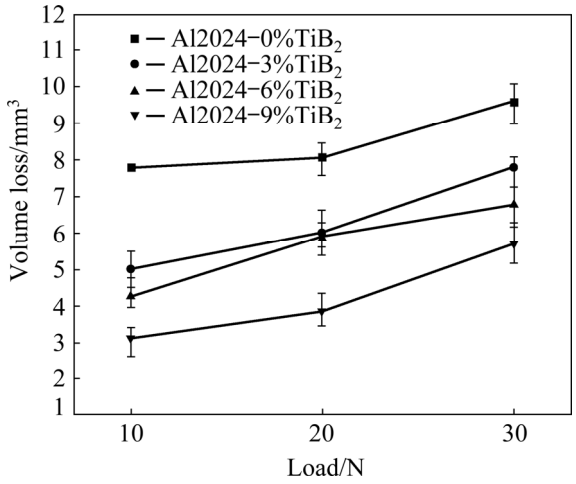

Fig. 3 Influence of load on volume loss of Al2024−TiB_2 composites

penetration of asperities, which accelerates the formation of metallic oxide, leading to smaller debris formation. Further increase in reinforcement content increases the intensity to resist the penetration of asperities, resulting in increase of wear resistance [31]. From Fig. 3, it can also be observed that volume loss of Al2024−3%TiB_2 and Al2024−6%TiB_2 composites at load 20 N are almost same, due to the adhesion of debris into the valley of the disc, resulting in higher material removal in the case of Al2024−6%TiB_2 composite at a load of 20 N.

Figure 4 displays the SEM images and EDS spectra of wear tracks of Al2024−TiB_2 composites at 10 N load, 0.5 m/s sliding velocity and 1800 m

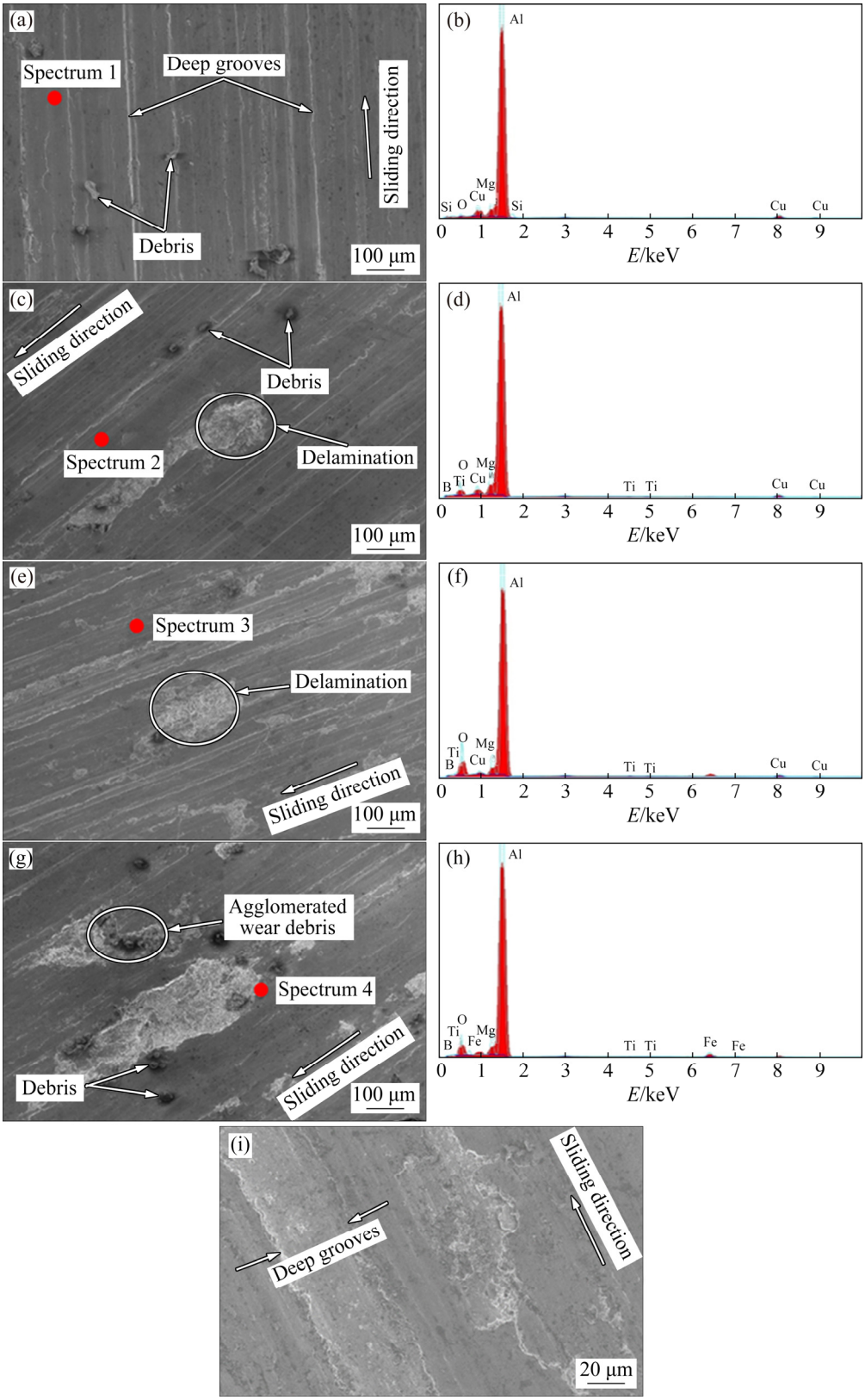

Fig. 4 SEM images (a, c, e, g, i) and EDS spectra (b, d, f, h) of wear tracks of Al2024−0%TiB_2 (a, b), Al2024−3%TiB_2 (c, d), Al2024−6%TiB_2 (e, f), Al2024−9%TiB_2 (g, h) composites and deep groove (i) in wear tracks of Al2024−0%TiB_2

sliding distance. From Figs. 4(a, c, e, g), it can be noticed that the morphologies of wear tracks of reinforced composites are different from matrix alloy. Unreinforced material exhibits deeper grooves on the wear tracks, whereas delamination and finer grooves are found in reinforced

composites. Thus, it can be concluded that, wear rate of Al2024 alloy is more compared to that of the reinforced composites. Further, wear track of Al2024−9%TiB_2 composite shows the existence of agglomeration of wear debris (Fig. 4(g)). Figure 4(h) depicts the existence of iron peak in Al2024−9%TiB_2 composite. This is because hardness of TiB_2 particles is more than that of the disc, which facilitates ploughing of material from the disc. This iron particle may get oxidized because of high frictional heat and form a layer (mechanically mixed layer), which acts as a lubricating film, thus enhancing the wear resistance. Figure 4(i) shows the existence of deep groove in the case of unreinforced material, which confirms the occurrence of higher material removal.

Figure 5 shows the SEM images and EDS spectra of wear debris of Al2024−TiB_2 composites at 10 N load, 0.5 m/s sliding velocity and 1800 m sliding distance. It can be noticed that the debris

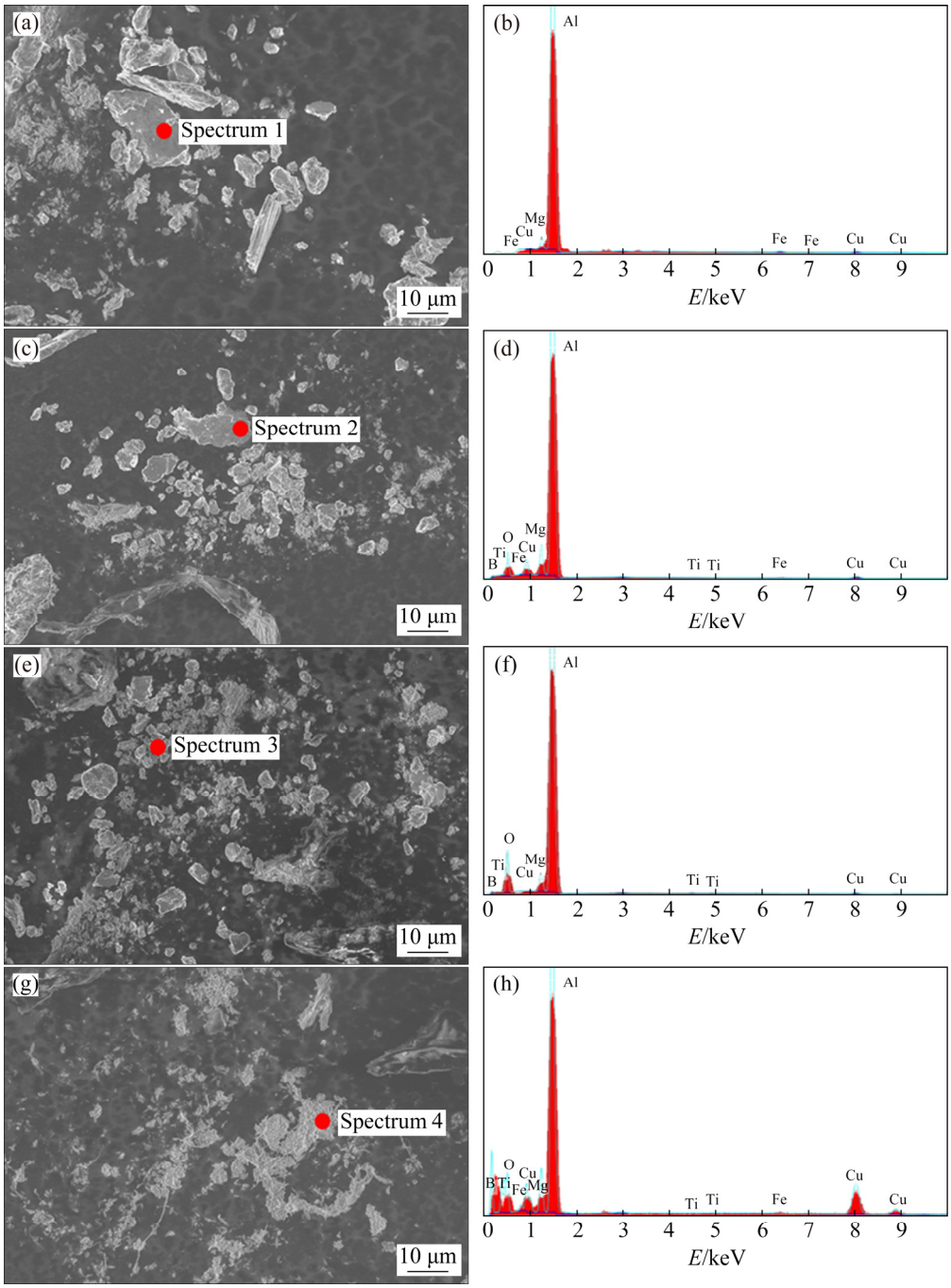

Fig. 5 SEM images (a, c, e, g) and EDS spectra (b, d, f, h) of wear debris of Al2024−0%TiB_2 (a, b), Al2024−3%TiB_2 (c, d), Al2024−6%TiB_2 (e, f) and Al2024−9%TiB_2 (g, h) composites

generated from unreinforced material is relatively large and is of irregular profiles (Fig. 5(a)). This type of debris is formed due to abrasive micro cutting. Whereas, smaller debris is generated in the case of reinforced composites (Figs. 5(c, e, g)). Furthermore, the size of wear debris becomes smaller with increase in TiB_2 content. This can be attributed to two reasons: the reduction in micro cutting and hardness enhancement with TiB_2 addition. From Figs. 5(b, d, f, h) it can be noticed that, Fe peaks are present in the EDS spectra (except for Al2024−6%TiB_2 composites) and its content is higher in reinforced composites compared to unreinforced material. This can be attributed to the abrasion of steel disc by the hard asperities.

Figure 6 displays SEM images of the wear tracks of Al2024−9%TiB_2 composite at different loads (10, 20 and 30 N), sliding velocity of 1.5 m/s and sliding distance of 1800 m. It can be noted that, material removal took place by delamination and plastic deformation (abrasive wear). Increase in load leads to the generation of high frictional heat between the pin sliding face and disc, which changes the grooves from fine to distinct. Further generation of craters and pits are also noticed. These are the signs of severe deformation contributing to a high rate of wear at higher loads.

Figure 7 displays SEM images of the wear debris of Al2024−9%TiB_2 composite at different loads (10, 20 and 30 N), sliding velocity of 1.5 m/s and sliding distance of 1800 m. Figure 7 shows that, increase in load results in an increase in wear debris size. Thus, it can be concluded that the wear rate rises with increase in load. Furthermore, at high loads both coarse and fine debris is observed. Existence of fine debris is due to the collapse of coarse debris owing to increased contact between sliding faces at higher loads.

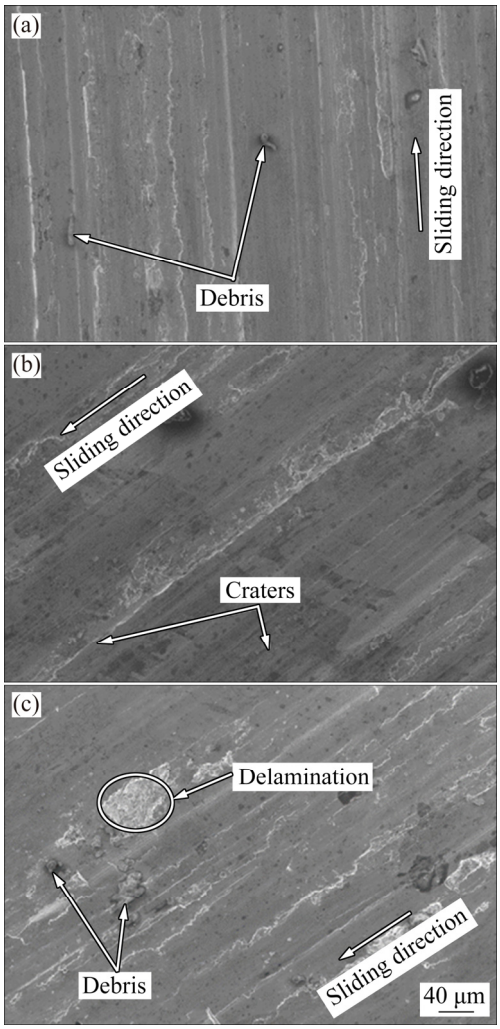

Fig. 6 SEM images of wear tracks of Al2024−9%TiB_2 composite at different loads: (a) 10 N; (b) 20 N; (c) 30 N

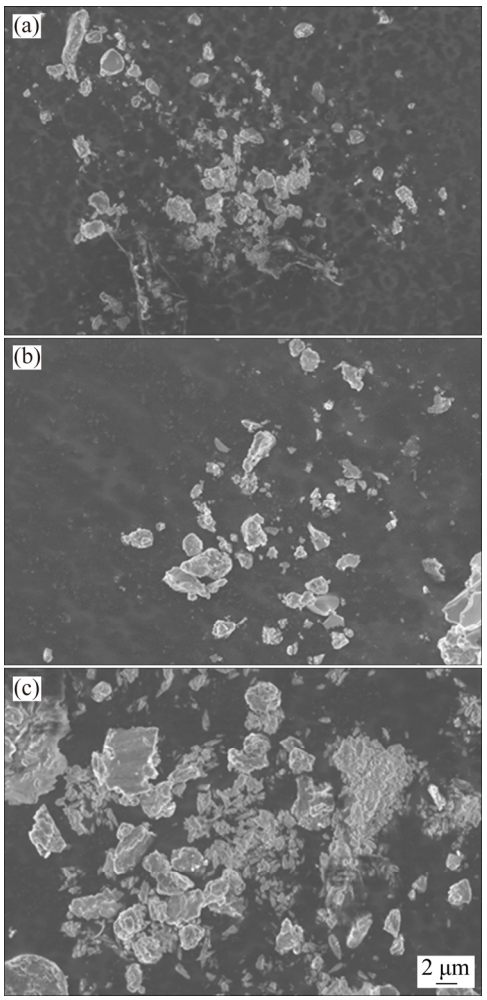

Fig. 7 SEM images of wear debris of Al2024−9%TiB_2 composite at different loads: (a) 10 N; (b) 20 N; (c) 30 N

3.2.2 Impact of sliding velocity

The wear tests were performed at three different sliding velocities (0.5, 1.0 and 1.5 m/s), keeping the applied load and sliding distance constant at 10 N and 1800 m, respectively. Figure 8 shows the influence of sliding velocity on volume loss of Al2024−TiB_2 composites. From Fig. 8, it can be observed that, with increase in sliding velocity, volume loss of Al2024−TiB_2 composites rises. Increase in sliding velocity promotes high frictional heat between the pin sliding face and disc. A higher degree of frictional heat softens the material, leading to weakening of matrix−reinforcement bonding. This weakening of matrix−reinforcement bonding facilitates material removal by digging the pin sliding face by hard asperities. Additionally, at constant load, high sliding velocity generates high shear stress between the pin and disc contact areas and because of this high shear stress, fragmentation of hard asperities occurs, leading to delamination of materials in the form of debris, thus resulting in increase in the wear rate [28,31,32]. Figure 8 also shows that volume loss of the matrix alloy is higher compared to that of the prepared composites. This might be because, the inclusion of TiB_2 particles facilitates grain refinement, which increases the dislocation density at the matrix−reinforcement interfaces, thus in turn increases the hardness, resulting in decrease in volume loss [24,33]. Increase in wear rate of Al2024−9%TiB_2 composite is moderate in comparison with other composites because of the improvement in strength and hardness with incorporation of TiB2 particles.

3.2.3 Impact of sliding distance

The wear tests were performed at three different sliding distances (900, 1800 and 2700 m), keeping the sliding velocity and load constant at 1.5 m/s and 10 N, respectively. Figure 9 shows the influence of sliding distance on volume loss of Al2024−TiB_2 composites. From Fig. 9, it can be noticed that with increase in sliding distance, volume loss of Al2024−TiB_2 composites rises and the behaviour is almost linear. Increase in the wear rate with rise in sliding distance is due to more surface contact between the sliding faces with prolonging time. As a consequence of this, temperature of the pin sliding face increases, therefore the material is softened, resulting in plastic deformation, thus increasing the wear rate [34]. The relation between sliding distance and volume loss can be better understood by the Archard's equation:

$$V=kPL/H \quad (2)$$

where k is a dimensionless constant, P is the load applied, L is sliding distance and H is the surface hardness. From Eq. (2), it is evident that volume loss is linearly proportional to sliding distance and inversely dependent on material hardness. High hardness of TiB_2 particles is also a contributing factor to the wear resistance, as it resists plastic deformation resulting in decrease of wear rate [22]. Figure 9 further depicts that with increase in mass fraction of TiB_2, wear resistance of Al2024−TiB_2 composites increases. Due to prolonged sliding action, the deformation of few hard asperities present in pin takes place and these asperities get detached from pin and adhere to the disc sliding face in the form of debris. During sliding, the debris acts as a stuffing material for the ditch created during experimental run, thus reducing the volume loss and contributing positively to wear resistance [31].

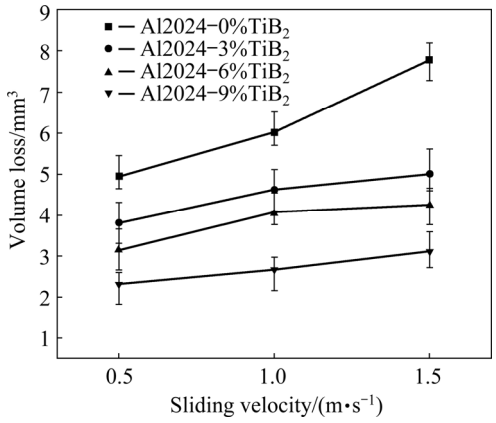

Fig. 8 Influence of sliding velocity on volume loss of Al2024−TiB_2 composites

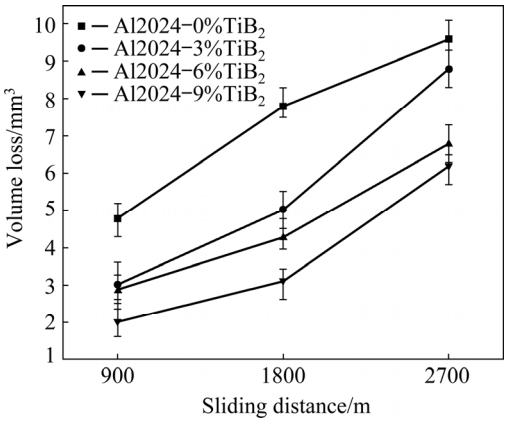

Fig. 9 Influence of sliding distance on volume loss of Al2024−TiB_2 composites

3.3 Coefficient of friction

3.3.1 Impact of load

Figure 10 represents the influence of applied load on coefficient of friction of Al2024−TiB_2 composites. From Fig. 10, it can be noticed that with increase in load, coefficient of friction of Al2024−TiB_2 composites decreases. At low loads, friction coefficient of unreinforced as well as reinforced composites is relatively high. This is because at low load, temperature on the contact surfaces between the pin and disc is also low, which does not facilitate oxide formation, leading to initiation of adhesion and abrasion between the contact asperities, resulting in higher coefficient of friction. But when load rises, temperature of the contact surfaces also increases. The increase in temperature accelerates the development of oxide layer between the contact surfaces. This oxide layer reduces the pin−disc contact, leading to low adhesion, resulting in reduction in coefficient of friction [33]. Another explanation for minimization of friction coefficient at higher loads is the trapping of large quantity of debris between the contact surfaces. Furthermore, the rise in temperature at higher loads results in fragmentation of asperities. The fragmented asperities may form a very fine molten layer between the sliding faces, which acts as a lubricating medium during sliding. Existence of this layer reduces the shear stress between the sliding surfaces, which in turn reduces the coefficient of friction [31].

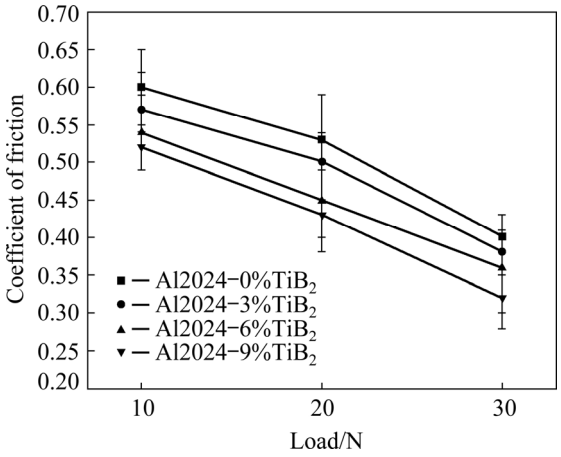

Fig. 10 Influence of load on coefficient of friction of Al2024−TiB_2 composites

However, the friction coefficient of all the fabricated composites is less than that of Al2024 matrix alloy under all load conditions. This indicates that friction property of Al2024 alloy is modified by the incorporation of TiB_2 particles, and this could be attributed to smaller particle sizes, clear interface and good dispersion. Uniform distribution of TiB_2 particles promotes excellent matrix− reinforcement bonding, which enriches the load- bearing capacity, thus contributing to magnificent anti-frictional behaviour [28]. It has also been reported that TiB_2 decreases the friction coefficient more efficiently than SiC [29].

3.3.2 Impact of sliding velocity

Figure 11 shows the influence of sliding velocity on friction coefficient of Al2024−TiB_2 composites. It can be seen from Fig. 11 that with increase in sliding velocity, friction coefficient of Al2024−TiB_2 composites increases. The increase in friction coefficient of Al2024−TiB_2 composites can be ascribed to the fact that, sliding velocity generates high frictional force between sliding faces of the pin and disc. As a consequence of this, hard asperities present in the composite crack and adhere to the sliding surfaces, acting like a lubricating film. At high sliding velocities, this lubricating film gets thickened. Further thickening of the lubricating film results in fragmentation. This fragmented film gets clogged onto the mating surfaces, resulting in higher coefficient of friction [28].

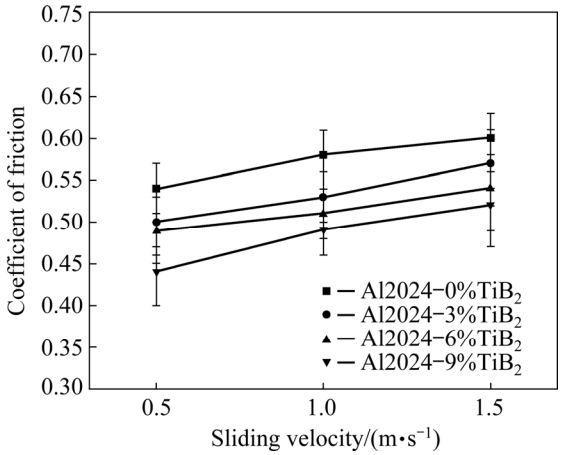

Fig. 11 Influence of sliding velocity on coefficient of friction of Al2024−TiB_2 composites

3.3.3 Impact of sliding distance

Figure 12 shows the impact of sliding distance on coefficient of friction of Al2024−TiB_2 composites. From Fig. 12, it can be depicted that with increase in sliding distance, the friction coefficient of Al2024−TiB_2 composites increases. The increase in the friction coefficient of

Al2024−TiB_2 composites with increase in sliding distance can be due to the upsurge in temperature between mating surfaces of the pin and disc, resulting in high frictional force [28]. However, friction coefficient of the fabricated composites reduces with increase in TiB_2 content for all sliding distances investigated.

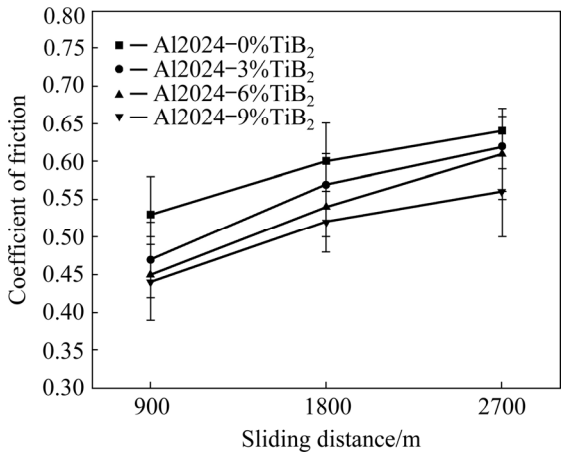

Fig. 12 Influence of sliding distance on coefficient of friction of Al2024−TiB_2 composites

Factors influencing the coefficient of friction are mechanical properties of matrix material, composition, hardness and chemical stability of reinforcement particles, matrix−reinforcement bonding and tribological parameters [29].

4 Conclusions

(1) Al2024−TiB_2 composites were successfully fabricated by stir casting process, with uniform dispersion of TiB_2 particles and good matrix−reinforcement bonding.

(2) Wear resistance of Al2024 matrix alloy is definitely increased by the incorporation of TiB_2 particles.

(3) Low friction and wear rates were observed in the developed composites compared to Al2024 matrix alloy, whereas wear rates of both Al2024 matrix alloy and fabricated composites increase with increase in load, sliding velocity as well as sliding distance.

(4) The friction coefficients of both Al2024 matrix alloy and fabricated composites reduce with increase in load, but rise with increase in sliding velocity and sliding distance.

(5) SEM analysis of worn surfaces depicts that delamination, adhesive and abrasive wear are present with delamination wear being predominant.

(6) Size of the wear debris plays a crucial role in ascertaining the wear rates of both Al2024 matrix alloy and fabricated composites.

References

[1] MALLIKARJUNA C, SHASHIDHARA S M, MALLIK U S, PARASHIVAMURTHY K I. Grain refinement and wear properties evaluation of aluminum alloy 2014 matrix−TiB_2 in-situ composites [J]. Materials & Design, 2011, 32: 3554−3559.

[2] HUANG W M, LIU B, WANG M L, LIU Y, WANG H W, MA N H. Study on the initial electrodeposition behavior of aluminum on TiB_2/A356 composite [J]. Materials and Corrosion, 2014, 65: 502−508.

[3] AKBARI M K, BAHARVANDI H R, SHIRVANIMOGHADDAM K. Tensile and fracture behavior of nano/micro TiB_2 particle reinforced casting A356 aluminum alloy composites [J]. Materials & Design, 2015, 66: 150−161.

[4] RAJAN H M, RAMABALAN S, DINAHARAN I, VIJAY S J. Synthesis and characterization of in situ formed titanium diboride particulate reinforced AA7075 aluminum alloy cast composites [J]. Materials & Design, 2013, 44: 438−445.

[5] AKHTAR F. Microstructure evolution and wear properties of in situ synthesized TiB_2 and TiC reinforced steel matrix composites [J]. Journal of Alloys and Compounds, 2008, 459: 491−497.

[6] KUMAR A, LAL S, KUMAR S. Fabrication and characterization of A359/Al_2O_3 metal matrix composite using electromagnetic stir casting method [J]. Journal of Materials Research and Technology, 2013, 2: 250−254.

[7] KARANTZALIS A E, WYATT S, KENNEDY A R. The mechanical properties of Al−TiC metal matrix composites fabricated by a flux-casting technique [J]. Materials Science and Engineering A, 1997, 237: 200−206.

[8] DEY D, CHINTADA S K, BHOWMIK A, BISWAS A. Evaluation of wear performance of Al2024−SiC ex-situ composites [J]. Materials Today: Proceedings, 2020, 26: 2996−2999.

[9] DEY D, BHOWMIK A, BISWAS A. Wear behavior of stir casted aluminum−titanium diboride (Al2024−TiB_2) composite [J]. Materials Today: Proceedings, 2020, 26: 1203−1206.

[10] SHIRVANIMOGHADDAM K, KHAYYAM H, ABDIZADEH H, AKBARI M K, PAKSERESHT A H, GHASALI E, NAEBE M. Boron carbide reinforced aluminium matrix composite: Physical, mechanical characterization and mathematical modelling [J]. Materials Science and Engineering A, 2016, 658: 135−149.

[11] SIVAPRASAD K, BABU S K, NATARAJAN S, NARAYANASAMY R, KUMAR B A, DINESH G. Study on abrasive and erosive wear behaviour of Al6063/TiB_2 in situ

composites [J]. Materials Science and Engineering A, 2008, 498: 495−500.

[12] SINGH G, CHAN S L I, SHARMA N. Parametric study on the dry sliding wear behaviour of AA6082−T6/TiB_2 in situ composites using response surface methodology [J]. Journal of the Brazilian Society of Mechanical Sciences and Engineering, 2018, 40: 310−322.

[13] BOOPATHI M M, ARULSHRI K P, IYANDURAI N. Evaluation of mechanical properties of aluminium alloy 2024 reinforced with silicon carbide and fly ash hybrid metal matrix composites [J]. American Journal of Applied Sciences, 2013, 10: 219−229.

[14] KURAPATI V B, KOMMINENI R, SUNDARRAJAN S. Statistical analysis and mathematical modeling of dry sliding wear parameters of 2024 aluminium hybrid composites reinforced with fly ash and SiC particles [J]. Transactions of the Indian Institute of Metals, 2018, 71: 1809−1825.

[15] KUMAR N, GAUTAM G, GAUTAM R K, MOHAN A, MOHAN S. Synthesis and characterization of TiB_2 reinforced aluminium matrix composites: A review [J]. Journal of the Institution of Engineers (India): Series D, 2016, 97: 233−253.

[16] PAZHOUHANFAR Y, EGHBALI B. Microstructural characterization and mechanical properties of TiB_2 reinforced Al6061 matrix composites produced using stir casting process [J]. Materials Science and Engineering A, 2018, 710: 172−180.

[17] LI P B, CHEN T J, QIN H. Effects of mold temperature on the microstructure and tensile properties of SiC_p/2024 Al-based composites fabricated via powder thixoforming [J]. Materials & Design, 2016, 112: 34−45.

[18] AKBARI M K, MIRZAEE O, BAHARVANDI H R. Fabrication and study on mechanical properties and fracture behavior of nanometric Al_2O_3 particle-reinforced A356 composites focusing on the parameters of vortex method [J]. Materials & Design, 2013, 46: 199−205.

[19] PORIA S, SAHOO P, SUTRADHAR G. Tribological characterization of stir-cast aluminium−TiB_2 metal matrix composites [J]. Silicon, 2016, 8: 591−599.

[20] SINGH J, CHAUHAN A. Fabrication characteristics and tensile strength of novel Al2024/SiC/red mud composites processed via stir casting route [J]. Transactions of Nonferrous Metals Society of China, 2017, 27: 2573−2586.

[21] JOHNY JAMES S, VENKATESAN K, KUPPAN P, RAMANUJAM R. Comparative study of composites reinforced with SiC and TiB_2 [J]. Procedia Engineering, 2014, 97: 1012−1017.

[22] TJONG S C, LAU K C. Dry sliding wear of TiB_2 particle reinforced aluminium alloy composites [J]. Materials science and technology, 2000, 16: 99−102.

[23] RADHIKA N, RAGHU R. Study on three-body abrasive wear behavior of functionally graded Al/TiB_2 composite using response surface methodology [J]. Particulate Science and Technology, 2018, 36: 816−823.

[24] MAHAMANI A, JAYASREE A, MOUNIKA K, PRASAD K R, SAKTHIVELAN N. Evaluation of mechanical properties of AA6061−TiB_2/ZrB_2 in-situ metal matrix composites fabricated by K_2TiF_6−KBF_4−K_2ZrF_6 reaction system [J]. International Journal of Microstructure and Materials Properties, 2015, 10: 185−200.

[25] SURESH S, MOORTHI N S V. Process development in stir casting and investigation on microstructures and wear behavior of TiB_2 on Al6061 MMC [J]. Procedia Engineering, 2013, 64: 1183−1190.

[26] MANDAL A, CHAKRABORTY M, MURTY B S. Effect of TiB_2 particles on sliding wear behaviour of Al−4Cu alloy [J]. Wear, 2007, 262: 160−166.

[27] KUMAR S, CHAKRABORTY M, SARMA V S, MURTY B S. Tensile and wear behaviour of in situ Al−7Si/TiB_2 particulate composites [J]. Wear, 2008, 265: 134−142.

[28] RAMESH C S, AHAMED A. Friction and wear behaviour of cast Al6063 based in situ metal matrix composites [J]. Wear, 2011, 271: 1928−1939.

[29] ZHAO M, WU G H, JIANG L T, DOU Z Y. Friction and wear properties of TiB_{2P}/Al composite [J]. Composites Part A: Applied Science and Manufacturing, 2006, 37: 1916−1921.

[30] RAO J B, RAO D V, PRASAD K S, BHARGAVA N R M R. Dry sliding wear behaviour of fly ash particles reinforced AA2024 composites [J]. Materials Science (Poland), 2012, 30: 204−211.

[31] SINGH R, SHADAB M, DASH A, RAI R N. Characterization of dry sliding wear mechanisms of AA5083/B_4C metal matrix composite [J]. Journal of the Brazilian Society of Mechanical Sciences and Engineering, 2019, 41: 98−109.

[32] HAMID A A, GHOSH P K, JAIN S, RAY S. The influence of porosity and particles content on dry sliding wear of cast in situ Al(Ti)−Al_2O_3 (TiO_2) composite [J]. Wear, 2008, 265: 14−26.

[33] DEY D, BISWAS A. Comparative study of physical, mechanical and tribological properties of Al2024 alloy and SiC−TiB_2 composites [J]. Silicon, 2020. https://doi.org/10.1007/s12633-020-00560-9.

[34] HUTCHINGS I M. Tribological properties of metal matrix composites [J]. Materials Science and Technology, 1994, 10: 513−517.

二硼化钛对 Al2024−TiB_2 非原位复合材料摩擦磨损性能的影响

Dipankar DEY, Abhijit BHOWMIK, Ajay BISWAS

Mechanical Engineering Department, NIT Agartala, Tripura-799046, India

摘　要：用搅拌铸造法制备不同质量分数二硼化钛(TiB_2)颗粒增强的铝基复合材料，并研究其摩擦磨损性能。采用销−盘式摩擦试验机对 Al2024−TiB_2 复合材料进行干滑动磨损试验。为了研究摩擦学参数对复合材料的影响，对载荷、滑动距离和滑动速度等参数进行调整。显微组织表征结果表明，TiB_2 颗粒分散均匀并与基体有良好的结合。实验结果表明，与 Al2024 合金相比，复合材料的摩擦磨损率更低，而 Al2024 合金和复合材料的磨损率均随载荷、滑动速度和滑动距离的增加而增加。然而，Al2024 合金和复合材料的摩擦因数均随载荷的增大而减小，而随滑动速度和滑动距离的增大而增大。对磨损表面和磨屑的扫描电镜研究表明，耐磨性的提高归因于细小磨屑的形成。

关键词：Al2024 合金；TiB_2；搅拌铸造；摩擦；磨损

(Edited by Wei-ping CHEN)